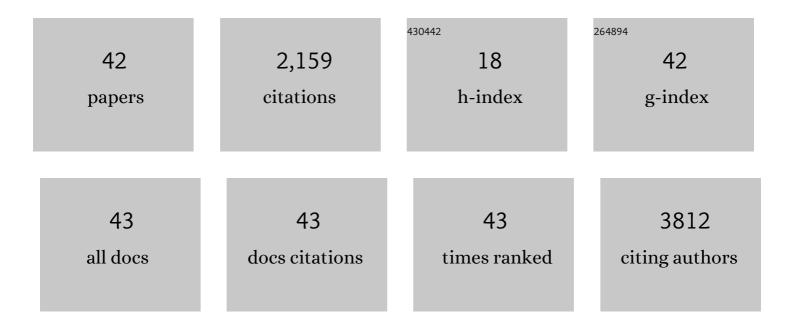
Yuan Huang

List of Publications by Year in descending order

Source: https://exaly.com/author-pdf/2721657/publications.pdf Version: 2024-02-01



ΥΠΑΝ ΗΠΑΝΟ

#	Article	IF	CITATIONS
1	Construction of an n-Body Potential for Revealing the Atomic Mechanism for Direct Alloying of Immiscible Tungsten and Copper. Materials, 2021, 14, 5988.	1.3	11
2	Highly sensitive non-enzymatic hydrogen peroxide monitoring platform based on nanoporous gold <i>via</i> a modified solid-phase reaction method. RSC Advances, 2021, 11, 36753-36759.	1.7	4
3	Enhanced Electrocatalytic Activities toward the Ethanol Oxidation of Nanoporous Gold Prepared via Solid-Phase Reaction. ACS Applied Energy Materials, 2020, 3, 336-343.	2.5	22
4	Collective and individual impacts of the cascade doping of alkali cations in perovskite single crystals. Journal of Materials Chemistry C, 2020, 8, 15351-15360.	2.7	1
5	Microscopic Investigation of High-Temperature Oxidation of hcp-ZrAl2. Oxidation of Metals, 2020, 94, 431-445.	1.0	1
6	Carrier transport composites with suppressed glass-transition for stable planar perovskite solar cells. Journal of Materials Chemistry A, 2020, 8, 14106-14113.	5.2	18
7	Influence of Al Addition Upon the Microstructure and Mechanical Property of Dual-Phase 9Cr-ODS Steels. Metals and Materials International, 2019, 25, 168-178.	1.8	7
8	Ultra-fine W–Y2O3 composite powders prepared by an improved chemical co-precipitation method and its interface structure after spark plasma sintering. Tungsten, 2019, 1, 220-228.	2.0	23
9	Effects of Zr Addition on Thermodynamic and Kinetic Properties of Liquid Mg-6Zn-xZr Alloys. Metals, 2019, 9, 607.	1.0	6
10	A Thermodynamically Favored Crystal Orientation in Mixed Formamidinium/Methylammonium Perovskite for Efficient Solar Cells. Advanced Materials, 2019, 31, e1900390.	11.1	101
11	Effect of deformation twinning on high-temperature performance of cold-rolled S31042 steel. Journal of Iron and Steel Research International, 2019, 26, 704-711.	1.4	2
12	Formation mechanisms of Y–Al–O complex oxides in 9Cr-ODS steels with Al addition. Journal of Materials Science, 2019, 54, 7893-7907.	1.7	15
13	Characterization of 14Cr ODS Steel Fabricated by Spark Plasma Sintering. Metals, 2019, 9, 200.	1.0	13
14	Helium bubble evolution and deformation of single crystal α-Fe. Journal of Materials Science, 2019, 54, 1785-1796.	1.7	8
15	A Eu ³⁺ -Eu ²⁺ ion redox shuttle imparts operational durability to Pb-I perovskite solar cells. Science, 2019, 363, 265-270.	6.0	793
16	Effects of aluminum and titanium on the microstructure of ODS steels fabricated by hot pressing. International Journal of Minerals, Metallurgy and Materials, 2018, 25, 1156-1165.	2.4	8
17	Uniformly Dispersed Freestanding Carbon Nanofiber/Graphene Electrodes Made by a Scalable Biological Method for Highâ€Performance Flexible Supercapacitors. Advanced Functional Materials, 2018, 28, 1803075.	7.8	83
18	The Exploration of Carrier Behavior in the Inverted Mixed Perovskite Singleâ€Crystal Solar Cells. Advanced Materials Interfaces, 2018, 5, 1800224.	1.9	58

Yuan Huang

#	Article	IF	CITATIONS
19	Novel Bacterial Cellulose/Gelatin Hydrogels as 3D Scaffolds for Tumor Cell Culture. Polymers, 2018, 10, 581.	2.0	43
20	Controlled Synthesis and Photocatalytic Performance of Au@ZnO Nanospheres with Core–Shell and Yolk-Shell Structures Assisted by Carbonaceous Layers as Intermediate. Journal of Nanoscience and Nanotechnology, 2018, 18, 2555-2561.	0.9	2
21	Chemical Reduction of Intrinsic Defects in Thicker Heterojunction Planar Perovskite Solar Cells. Advanced Materials, 2017, 29, 1606774.	11.1	318
22	Sacrificial template method for the synthesis of three-dimensional nanofibrous 58S bioglass scaffold and its inÂvitro bioactivity and cell responses. Journal of Biomaterials Applications, 2017, 32, 265-275.	1.2	22
23	The intrinsic properties of FA _(1â^'x) MA _x PbI ₃ perovskite single crystals. Journal of Materials Chemistry A, 2017, 5, 8537-8544.	5.2	152
24	Hot deformation behavior and microstructural evolution of Nb–V–Ti microalloyed ultra-high strength steel. Journal of Materials Research, 2017, 32, 3777-3787.	1.2	13
25	Formation of Fine B2/l̂²Â+ÂO Structure and Enhancement of Hardness in the Aged Ti2AlNb-Based Alloys Prepared by Spark Plasma Sintering. Metallurgical and Materials Transactions A: Physical Metallurgy and Materials Science, 2017, 48, 4365-4371.	1.1	18
26	Induction of diffusion and construction of metallurgical interfaces directly between immiscible Mo and Ag by irradiation-induced point defects. RSC Advances, 2017, 7, 53763-53769.	1.7	3
27	Austenite to polygonal-ferrite transformation and carbide precipitation in high strength low alloy steel. International Journal of Materials Research, 2017, 108, 12-19.	0.1	2
28	The Progress of Interface Design in Perovskiteâ€Based Solar Cells. Advanced Energy Materials, 2016, 6, 1600460.	10.2	139
29	Hydrogenated nanoporous TiO2 film on Ti 25Nb 3Mo 2Sn 3Zr alloy with enhanced photocatalytic and sterilization activities driven by visible light. Journal of Alloys and Compounds, 2016, 678, 5-11.	2.8	18
30	Effects of cold rolling on the precipitation and the morphology of δ-phase in Inconel 718 alloy. Journal of Materials Research, 2016, 31, 443-454.	1.2	14
31	Preparation of nanoporous molybdenum film by dealloying an immiscible Mo–Zn system for hydrogen evolution reaction. RSC Advances, 2016, 6, 15390-15393.	1.7	16
32	Oxygen-vacancy modified TiO ₂ nanoparticles as enhanced visible-light driven photocatalysts by wrapping and chemically bonding with graphite-like carbon. RSC Advances, 2016, 6, 10887-10894.	1.7	12
33	Tribological behavior of threeâ€dimensional braided carbon fiber reinforced polyetheretherketone composites. Polymer Composites, 2015, 36, 2174-2183.	2.3	6
34	Au@Cu ₇ S ₄ yolk–shell nanoparticles as a 980 nm laser-driven photothermal agent with a heat conversion efficiency of 63%. RSC Advances, 2015, 5, 87903-87907.	1.7	34
35	FABRICATION AND CHARACTERIZATION OF NOVEL Fe–Ni ALLOY COATED CARBON FIBERS FOR HIGH-PERFORMANCE SHIELDING MATERIALS. Surface Review and Letters, 2015, 22, 1550028.	0.5	4
36	Controlled delivery of dexamethasone from TiO2 film with nanoporous structure on Ti–25Nb–3Mo–2Sn–3Zr biomedical alloy without polymeric carrier. Materials Letters, 2014, 128, 384-387.	1.3	11

Yuan Huang

#	Article	IF	CITATIONS
37	Yolk–shell structured Fe3O4@C@F-TiO2 microspheres with surface fluorinated as recyclable visible-light driven photocatalysts. Applied Catalysis B: Environmental, 2014, 150-151, 515-522.	10.8	48
38	Self-organizing evolution of anodized oxide films on Ti-25Nb-3Mo-2Sn-3Zr alloy and hydrophilicity. Transactions of Tianjin University, 2014, 20, 97-102.	3.3	1
39	Fabrication of Ge quantum dots doped TiO2 films with high optical absorption properties via layer-by-layer ion-beam sputtering. Materials Letters, 2012, 67, 369-372.	1.3	15
40	Three-dimensional cuprous oxide microtube lattices with high catalytic activity templated by bacterial cellulose nanofibers. Journal of Materials Chemistry, 2011, 21, 10637.	6.7	44
41	Dynamic interaction between the growing Ca–P minerals and bacterial cellulose nanofibers during early biomineralization process. Cellulose, 2010, 17, 365-373.	2.4	35
42	Characterisation of Hydroxyapatite/Bacterial Cellulose Nanocomposites. Polymers and Polymer Composites, 2009, 17, 353-358.	1.0	14